Thermodynamical study of the interaction between clusters

F. Calvo
Laboratoire Collisions, Agregats, Réactivité (UMR 5589, CNRS), IRSAMC, Université Paul Sabatier, 118, Route de Narbonne, 31062 Toulouse Cedex, France

F. Spiegelmann
Laboratoire de Physique Quantique (UMR 5626, CNRS) IRSAMC, Université Paul Sabatier, 118, Route de Narbonne, 31062 Toulouse Cédex, France

(Received 22 May 1996)

We investigate the thermodynamical stability of the interaction between two clusters at thermal equilibrium using classical molecular-dynamics (MD) and Monte Carlo (MC) simulations. The intercluster distance Z is fixed as a parameter in the microcanonical and canonical ensembles. We use and develop several techniques to calculate the fundamental quantities of interest in these ensembles, namely, the density of states $\Omega(E,Z)$ and the partition function $Q(T,Z)$, yielding respectively, the microcanonical entropy $S(E,Z)$ and the Helmholtz free energy $F(T,Z)$. The multiple histogram method is used to estimate the variations of S with E and of F with T, both extracted from either constant energy MD or constant-temperature MC simulations. The thermodynamic perturbation and the displacement-vector methods are used to provide the variations of the free energy along the Z coordinate. These methods are applied to the interaction of $Ar_{13}+Ar_{13}$ and Na_8+Na_8 clusters. The Lennard-Jones $(Ar_{13})_2$ cluster dimer has a locally mechanically stable structure at $Z=8.6$ Å, which appears to remain thermodynamically stable until $T\simeq 25$ K. The temperature effects also stabilize two intermediate compact configurations, near $Z=5$ and 6.6 Å. On the other hand, the interaction between Na_8+Na_8, modeled by a distance-dependent tight-binding Hamiltonian, does not exhibit a stable structure except in its compact shape Na_{16}. The entropic effects, favored by the thermal phenomena, do not occur to induce any thermodynamical local stability for a dimerized $(Na_8)_2$. In other terms, the stability of Na_{16} does not seem to be governed by the underlying two Na_8 magic-number units. [S0163-1829(96)00939-3]

I. INTRODUCTION

On both experimental and theoretical sides, the interest of chemists and physicists in small clusters of atoms or molecules has increased constantly in the last decades. In particular, a great deal of attention was paid to their structural and thermodynamical properties. Among the different species of clusters, special interest has been paid to homogeneous rare-gas systems as prototypes of van der Waals clusters, and also to alkalis as the simplest example of metallic clusters.

Those two kinds of systems offer very different types of physics. Indeed, in rare-gas clusters, the electrons remain localized on the atoms, and no chemical bond is established (only weak van der Waals bonding). Conversely, the electrons in metallic clusters are strongly delocalized. Thus the rare-gas systems are well described with simple pair additive energy functions such as the Lennard-Jones (LJ) potential, whereas metallic systems must receive treatments allowing for electron delocalization, namely, more or less sophisticated explicit quantal treatments. Despite this strong physical difference, it occurs that the equilibrium geometrical configurations may present some common general features. The most stable isomers have generally compact shapes, and in both cases show arrangements around pentagonal or icosahedral patterns, at least in the range of a few tens of atoms.[1–4]

However, several studies have conjectured, in particular in the case of metallic clusters, the existence of clusters dimers. The existence of such deformed clusters was first investigated using the two-center jellium model,[5] and resumed by Knospe *et al.*[6] These authors calculated the potential-energy evolution with the intercluster distance for Na_n+Na_n, $n=8$, 9, 19, and 20. Na_8+Na_8 was shown to exhibit a stable local minimum for a separation of 13.5 bohr between the centers of mass of the two subunits. This corresponds to a very prolate structure. The more sophisticated results of cylindrically averaged pseudopotential scheme (CAPS) (Ref. 7) calculations of Na_{16} also reveal a ''superdeformed'' structure consisting of two Na_8 subunits. However, all of these studies assume or constrain a cylindrical symmetry. As a matter of fact, all three-dimensional calculations for Na_{16} tend to establish that it most probably exhibits a triaxial structure.[4,8,9]

The possibility of creating clusters dimers has also been investigated using a collisional approach,[6,10–12] necessarily dynamical. However, it is clear that, in a two-cluster collision, even if the incident cluster has a very small relative velocity, the system cannot be permanently stabilized due to the total-energy conservation. Thus it was concluded that a prolate Na_8+Na_8 cluster dimer may appear only as a transient species at the beginning of the collision, but that it decays into a compact form through a thermalization process. The lifetime of such a prolate complex seems to be more likely described by a continuous dissipation process resulting from a redistribution of relative collisional energy into thermal degrees of freedom, rather than a trapping in a well of the potential-energy surface (PES) corresponding to a stable dimerized deformed isomer. In fact no evidence of a barrier between a prolate structure and a compact isomer was

found along the reaction path in the work of Zhang and co-workers.[11,12] In any case, the stabilization of a cold cluster in a collision between two subunits requires an energy release through evaporation or fragmentation. Therefore it is difficult in such processes to probe the PES topography accurately.

It is possible to develop purely static approaches ($T=0$) to explore reaction paths or least-energy paths between isomers (chain algorithms or quenching procedures along the dynamical trajectory). However, in order to be exhaustive, these methods require an extensive sampling of the initial conditions, in particular the relative orientations of the velocities. Moreover, at finite temperature it is likely that not all the numerous local minima on the PES are very significant and need to be recorded. The entropic effects should also be taken into account in a consistent way. This is also to be related to the studies of phase changes and general thermodynamical behavior of such systems.[13–16] A pertinent description of the problem may consist in keeping the intercluster separation coordinate Z as an explicit deterministic parameter, while the other degrees of freedom receive a statistical treatment. In this line, the thermodynamical free-energy function $F(T,Z)$ seems to provide a relevant framework to describe the system.

In this paper, we address the general problem of the thermodynamical study of the X_p+X_q approach between two clusters (here $p=q$ and the total number of atoms is $N=2p$). Our purposes are (i) to establish the ability of different methodologies for computing the thermodynamical functions with a constraint parameter (here, the intercluster distance Z); and (ii) to examine the stability or unstability of cluster dimers at finite temperatures with respect to *free energies* calculated from a known reference state (here the two clusters at $Z=\infty$ and $T=0$).

The various theoretical and computational methods used and developed in this work are presented in Sec. II. In Sec. III, we discuss the results obtained with these methods applied to the stability of the $Ar_{13}+Ar_{13}$ problem as a direct application, taking advantage of the simplicity and computational efficiency of the Lennard-Jones pairwise potential modeling to achieve rather exhaustive sampling and significant statistics.

The same techniques are then applied to the thermodynamical study of the Na_8+Na_8 interaction with a distance-dependent tight-binding (DDTB) model. Although more sophisticated methods have been used in the literature to describe alkali-metal clusters, quantum chemistry calculations[17] and the local-density approximation (LDA),[18] those techniques are too computer-time consuming to be handled in quantitative thermodynamical sampling, even the LDA in the Car-Parrinello formulation. The present DDTB model was shown to provide energetic and geometrical properties in quantitative agreement with *ab initio* calculations when available. The application for Na_8+Na_8 is presented in Sec. IV. We finally compare the methodologies and discuss the results in Sec. V.

II. METHODS

As a preliminary step, we examine the situation at $T=0$. We systematically search the global minimum of the potential energy as a function of the intercluster separation Z, e.g., the mechanically stable clusters with the holonomic constraint $Z=$ const. Both global (simulated annealing and regular quenching along a collisional trajectory) and local (conjugate gradient or steepest descent) exploration methods are involved.

The methods for computing the free energy used or developped in the present paper can be sorted into two major categories:

(i) The first category is a finite temperature or finite energy search. It consists, at fixed $Z=Z_0$, of calculating the fundamental quantity of interest in the microcanonical and canonical ensembles, that is either the entropy $S(E,Z_0)$ or the free energy $F(T,Z_0)$. This was done with the multiple histogram method. This practically requires, for this given Z, to achieve microcanonical simulations in a range of energies or canonical simulations in a range of temperatures.

(ii) The second category is also a finite temperature calculation of the free energy $F(Z,T_0)$, but at fixed temperature T_0. It consists of estimating free energy differences along the Z coordinate, keeping the temperature at fixed value T_0.

We assume that the N-atom cluster dimer is described with a potential energy function V only dependent on the atoms or nuclei coordinates $\vec{R}=\{x_i,y_i,z_i\}$. We also assume that both clusters center of mass (c.o.m.) are aligned on the z axis, so that the intercluster distance Z, also considered as a function ξ of the coordinates, is calculated by

$$Z=\xi(\vec{R})=\frac{1}{M_B}\sum_{i\in B} m_i z_i-\frac{1}{M_A}\sum_{i\in A} m_i z_i \qquad (1)$$

where M_A and M_B are the total masses of the clusters A and B for the configuration $A+B$, and $\{m_i\}$ the individual atomic masses.

In general thermodynamical simulations, the choice between general algorithms like Monte Carlo (MC) or molecular dynamics (MD) is not of any special importance, since both MC and MD methods are known to be equivalent from the thermodynamical equilibrium point of view,[19] which is essential here. However, MD methods present several drawbacks from a practical point of view. First, they require the determination of the energy gradient along the simulation, which is time consuming, particularly with a quantal-type Hamiltonian. Moreover, MD simulations of geometrically constrained systems *at fixed temperature* must be implemented with intricate algorithms,[20,21] whereas MC methods are always more straightforward to handle. Following the evolution with real time is not crucial in the purpose of determining thermodynamical functions.

For the present application, the implementation of simulations with a holonomic constraint is made with two main methods. On the one hand, one can introduce an artificial constraint to keep Z at an initial value, via an extra potential $\tilde{V}(Z)$ added to the potential-energy function. This is the *umbrella sampling* method,[22,23] where $\tilde{V}(Z)$ is often harmonic. On the other hand, one can really constrain in time (or in Monte Carlo pseudotime) the system to remain on the hypersurface $Z=$ const. This last technique (the so-called *blue-moon* ensemble sampling[24]) introduces some correcting terms in the free energy when sampling this biased distribution of the phase space with molecular dynamics.[25] Actually,

a recent work by Depaepe *et al.*[26] showed that these two methods were equally valid and produced the same quantitative results. When choosing MC rather than MD sampling, one gets rid of extra calculations along the simulation (with respect to an unconstrained simulation) by preferring the blue-moon method to the umbrella sampling method, because the latter one is especially simple to implement in a MC framework.

To avoid the evaporation processes which may occur as soon as the temperature is high enough, we enclosed the dimer into an ellipsoid trap and added to the potential energy an extra harmonic term

$$V_{\rm rep}(\vec{R})=\sum_i \begin{cases} \kappa(r_A^i+r_B^i-d)^2/2, & r_A^i+r_B^i>d \\ 0, & r_A^i+r_B^i\leqslant d \end{cases} \tag{2}$$

with $\vec{R}=\{x_i,y_i,z_i\}$. r_A^i and r_B^i are the respective distances between the atom or nuclei i and the centers of mass of the clusters A and B, and $d=2Z+\sigma$. κ and σ are numerical constants, chosen in practice, respectively, as 100 times the atomic dimer energy and 2.3 times the interatomic averaged distance in the compact cluster. This ellipsoid wall was also used in MD simulations for argon, in order to be able to compare the results between MD and MC constrained simulations. In the following, the potential V implicitly includes this repulsive term.

A. Optimization methods at $T=0$

As a preliminary step toward the calculation of thermal quantities such as the free energy, the systematic search for locally stable structures with fixed Z constitutes an attempt to explore as exhaustively as possible the configurational space of the cluster dimer. In fact, here we deal only with a hypersurface at fixed Z of this space.

The global algorithm for finding at fixed Z the absolute minima on the PES is a simple Monte Carlo simulated annealing, forcing the constraint by keeping the c.o.m. of each subcluster unit fixed at each step, when performing independently collective MC moves. We have thus generally used the MC sampling. However, when applying the multiple histogram method (ii) in Sec. II B, we also compare MC and MD simulations.

For each Z, after the simulated annealing process was achieved and to avoid artifacts, we further locally optimized the obtained structure with a quenching procedure, based either on steepest descent or conjugate gradient algorithms.[27] The usual steepest descent quenching method minimizes the potential energy by carrying on consecutive steps along the gradient direction, and thus solves the equation $d\vec{r}_i/dt=-\alpha\vec{\nabla}_i V(\vec{R})$, with α a numerical parameter. With the Z constraint, one adds a Lagrange multiplier λ so that the potential energy becomes

$$V_{\lambda,Z}(\vec{R})=V(\vec{R})+\lambda[\xi(\vec{R})-Z]. \tag{3}$$

The artificial resulting ''forces'' (as part of the gradient) will insure the intercluster distance to remain fixed. By writing

$$\frac{\partial V_{\lambda,Z}}{\partial\lambda}=0, \tag{4}$$

$$\frac{\partial V_{\lambda,Z}}{\partial Z}=0, \tag{5}$$

we easily find propagation equations for the Z-constrained quenching procedure:

$$\frac{dx_i}{dt}=-\alpha\frac{\partial V}{\partial x_i}, \tag{6}$$

$$\frac{dy_i}{dt}=-\alpha\frac{\partial V}{\partial y_i}, \tag{7}$$

$$\frac{dz_i}{dt}=\begin{cases} -\alpha\dfrac{\partial V}{\partial z_i}+\alpha\dfrac{m_i}{M_A}\dfrac{\partial V}{\partial Z} & i\in A \\ -\alpha\dfrac{\partial V}{\partial z_i}-\alpha\dfrac{m_i}{M_B}\dfrac{\partial V}{\partial Z} & i\in B. \end{cases} \tag{8}$$

The calculation of $\partial V/\partial Z$ with respect to the clusters coordinates $\vec{R}=\{x_i,y_i,z_i\}$ is made explicit in Ref. 28, and gives the following equation:

$$\frac{\partial V}{\partial Z}=\frac{M_A}{M_A+M_B}\sum_{i\in B}\frac{\partial V}{\partial z_i}-\frac{M_B}{M_A+M_B}\sum_{i\in A}\frac{\partial V}{\partial z_i}. \tag{9}$$

This quenching procedure appears to be a very efficient and powerful tool for locating the bottoms of the PES wells with the Z constraint. It also allows the implementation of general dynamical algorithms such as conjugate gradient or classical molecular dynamics with this constraint, since the same Lagrange multiplier may be added to the Hamiltonian instead of only its configurational part. (For a general description on molecular dynamics with holonomic constraints, see Ref. 29.)

Starting either from the separated systems configuration X_p+X_q with large Z, or from the known compact structure X_{p+q} with minimal Z, the internuclear distance is changed to intermediate values, and simulated annealing is performed followed with local quenching. The resulting structures are the constitutive basis for the aftercoming thermal studies.

When starting from an initial long distance, the preliminary minimization of the energy with respect to the relative orientation of the (almost) separated clusters was solved specifically by performing several Monte Carlo simulations on the four ϕ_A, ψ_A, ϕ_B, and ψ_B spherical angles associated with the two clusters. This occured to be more practical in the case of argon, for which the uncut LJ potential is still active at long range.

Finally, a third method was employed to explore the small-Z region better, using periodic quenching along classical MD collision trajectories with thermalized initial velocities. We sometimes found some structures with this procedure which were lower than those obtained by artificially imposing the distance and then achieving optimization. This situation occured more frequently for sodium clusters.

The classical Metropolis algorithm[30] was used in MC simulations, and a fourth-order Runge-Kutta procedure propagated Hamilton's equations in MD simulations.

B. Constrained multiple histogram method

From now on we wish to estimate the microcanonical density of states $\Omega(E,Z)$ and the canonical partition function $Q(T,Z)$, which lead directly to the microcanonical entropy $S(E,Z)=k_B \ln\Omega(E,Z)$ and to the free energy of the cluster, $F(T,Z)=-k_B T \ln Q(T,Z)$, where k_B is Boltzmann's constant. The procedure for computing $\Omega(E,Z)$ and $Q(T,Z)$ at fixed Z is a multiple histogram method, adapted in the following for the Z constraint.

First used for clusters in a work of Labastie and Whetten who studied the solid-liquid transition in Mackay icosahedra argon clusters,[31] this method extracts from simulations the fundamental quantity from which all the thermodynamical data can be deduced; that is, the microcanonical density of states. The cluster community has used with benefit this method for studying thermal phenomena, mainly phase changes,[15,31,32] and evaporation in clusters.[33] Up to a recent work,[19] the histogram methods were restricted to constant-temperature simulations (either Monte Carlo[15,31,32] or Nosé molecular dynamics[33]). The extension of the method to isoenergetic MD simulations provided an efficient way to treat the thermodynamical equilibrium of an isolated cluster. Nevertheless, we also propose to calculate the density of states with the Z constraint, in the microcanonical ensemble. We describe successively the implementation of the formalism to MD and MC simulations. In MD simulations, the constraint is imposed through a Dirac δ function:

$$\Omega(E,Z)=\int_\Gamma \delta[\xi(\vec{R})-Z]\,\delta\left[\frac{d\xi(\vec{P})}{dt}\right]\delta[H(\vec{R},\vec{P})-E]\,d^{3N-6}\vec{R}\times d^{3N-6}\vec{P}, \tag{10}$$

$$Q(T,Z)=\int_\Gamma \delta[\xi(\vec{R})-Z]\,\delta\left[\frac{d\xi(\vec{P})}{dt}\right]\times\exp[-\beta H(\vec{R},\vec{P})]\,d^{3N-6}\vec{R}\times d^{3N-6}\vec{P} \tag{11}$$

Here Γ is the phase space and $3N-6$ is the total number of independent degrees of freedom of the cluster dimer. $H(\vec{R},\vec{P})$ is the Hamiltonian.

Let us now describe a system of coordinates $\{Z_G,Z,x_i,y_i,z_i'\}$, where Z_G is the coordinate of the dimer c.o.m., and z_i' is an atom or nucleus coordinate with respect to the c.o.m. of the cluster it belongs to. Since the global translation and rotation of the dimer do not influence the value of $\Omega(E,Z)$, we assume Z_G of no importance in the following. We then have

$$\Omega(E,Z)=\int_{\Gamma_Z'} J\,\delta[\xi(\vec{R}',Z)-Z]\,\delta\left[\frac{d\xi(\vec{P}',P_Z)}{dt}\right]\times\delta[H(\vec{R}',\vec{P}',Z,P_Z)-E]\,d\Gamma_Z'. \tag{12}$$

$\vec{R}'=\{x_i,y_i,z_i'\}$ is the representative configuration in the $3N-7$ manifold, and J is the Jacobian of the $\Gamma=\{\vec{R},\vec{P}\}\rightleftharpoons\Gamma_Z'=\{\vec{R}',\vec{P}',Z,P_Z\}$ transformation. P_Z is the conjugate momentum of Z, and the integration is performed with $d\Gamma_Z'=d^{3N-7}\vec{R}'\times d^{3N-7}\vec{P}'\times dZ\times dP_Z$. It can easily be shown that

$$P_Z=\frac{M_A}{M_A+M_B}\sum_{i\in B}p_{z_i}-\frac{M_B}{M_A+M_B}\sum_{i\in A}p_{z_i}=\frac{M_A M_B}{M_A+M_B}\xi(\vec{P}) \tag{13}$$

with p_{z_i} the conjugate momentum of z_i. Since this transformation is linear in the coordinates, J is a constant. The integration on Z and P_Z can be performed, and finally leads to

$$\Omega(E,Z)=J\frac{M_A+M_B}{M_A M_B}\int_{\Gamma'}\delta[K(\vec{P}')+V(\vec{R}',Z)-E]\,d^{3N-7}\vec{R}'\times d^{3N-7}\vec{P}' \tag{14}$$

with $K(\vec{P}')$ and $V(\vec{R}',Z)$ the respective kinetic and potential energies of the system, and where Γ' denotes the restricted $\{\vec{R}',\vec{P}'\}$ phase space. In the following, we do not take into account the factor $J(M_A+M_B)/M_A M_B$, since its contribution to the density of states is only a multiplicative constant. The following multiple histogram procedure is used to extract the $\Omega(E,Z)$ quantity from isoenergetic MD simulations.

We start from Eq. (14), which we write as

$$\Omega(E,Z)=\int_0^E \Omega_C(V,Z)\,\Omega_K(E-V)\,dV, \tag{15}$$

where $\Omega_K(E)$ is the kinetic density of states,

$$\Omega_K(E)=\frac{d}{dE}\int_{K(\vec{P}')\leqslant E} d^{3N-7}\vec{P}', \tag{16}$$

and $\Omega_C(V,Z)$ is the configurational density of states,

$$\Omega_C(V,Z)=\frac{d}{dV}\int_{V(\vec{R}',Z)\leqslant V} d^{3N-7}\vec{R}'. \tag{17}$$

The fact that Ω_K does not depend on the Z coordinate is indeed due to the linearity of the transformation, as discussed by Paci *et al.*[25] and by Depaepe *et al.*[26] Since this kinetic term has a simple expression as $\Omega_K(E)=\alpha E^{(3N-9)/2}$, Eq. (15) suggests a MD multiple histogram application to extract $\Omega_C(V,Z)$ at fixed Z. We say that, if a simulation at constant total energy $E=V+K$ is ergodic, the normalized probability distribution of V is

$$\rho_Z(V,E)=\frac{\Omega_K(E-V)\,\Omega_C(V,Z)}{\Omega(E)}. \tag{18}$$

So, if the simulation is performed with energy E_i, the probability density to have the potential energy V_j is given by

$$\rho_{ij}=\alpha_i\Omega_j(E_i-V_j)^{(3N-9)/2} \tag{19}$$

with $\Omega_j=\Omega_C(V_j,Z)$ and $\alpha_i=1/\Omega(E_i)$.

The multiple histogram method can then be applied to such an equation. It makes the extraction of $\Omega(E,Z)$ possible (for full details, see Refs. 15 and 19) from a series of simu-

lations at constant E, for the same value of Z. The only requirement is that the distributions of energies must overlap, in a similar way than in the umbrella sampling method.[22] From $\Omega(E,Z)$, one directly has $S(E,Z)$, up to a global additive constant corresponding to the freedom in choosing the entropy reference. This scheme can be used to calculate the configurational entropy of the separated configuration X_p+X_q, as a function of the total energy.

We now examine the case of the MC simulation scheme. In the canonical ensemble, the fundamental quantity is the partition function, Eq. (11). In the system of coordinates $\{\vec{R}',\vec{P}',Z,P_Z\}$, one has

$$Q(T,Z)=\int_{\Gamma'}\exp(-\beta[K(\vec{P}')+V(\vec{R}',Z)])d\vec{R}'\times d\vec{P}'. \tag{20}$$

Since $K(\vec{P}')$ does not depend on Z, Q can be factorized into its kinetic and configurational parts. The configuration integral $Q_C(T,Z)$ is defined as

$$Q_C(T,Z)=\int_{\Lambda'}e^{-\beta V(\vec{R}',Z)}d\vec{R}', \tag{21}$$

with $\Lambda'=\{\vec{R}'\}$ the restricted configurational space. As in the microcanonical ensemble, Eq. (21) has another expression in terms of the configurational density of states $\Omega_C(V,Z)$:

$$Q_C(T,Z)=\int_0^\infty \Omega_C(V,Z)\exp(-\beta V)dV. \tag{22}$$

To compute $\Omega_C(V,Z)$, we say that the probability of finding the Z-constrained cluster dimer in a configuration with energy V_i and at temperature T_j is given by the canonical distribution

$$\rho_{ij}=\Omega_C(V_i,Z_j)\exp(-\beta_j V_i)/Q(T_j,Z_i). \tag{23}$$

In the canonical ensemble, the multiple histogram method is applied to such an equation. $\Omega_C(V,Z)$ can then be calculated from a series of simulations at constant T, for the same value of Z. Again, the only requirement is that the distributions of energies must overlap. One then easily computes the configurational free energy $F_C(T,Z)$, up to a global additive constant. We chose the reference as $F_C(T=0,\ Z=\infty)=0$.

Once the density of states $\Omega(E,Z)$ is known either from MC or MD simulations, one can easily calculate the canonical partition function $Q(T,Z)$ by

$$Q(T,Z)=\int_0^\infty \Omega(E,Z)\exp\left(-\frac{E}{k_BT}\right)dE, \tag{24}$$

and a similar expression to calculate the configuration integral $Q_C(T,Z)$ from $\Omega_C(V,Z)$. Both MD and MC methods described above were used to compute both the configurational entropy $S_C(V,Z)$ and the partition function $Q_C(T,Z)$.

C. Direct calculation of $F_C(T,Z)$ at fixed T

We now present two methods to estimate directly configurational free-energy differences along the Z coordinate, keeping the temperature at fixed value. A first method chosen for this purpose is very general, and consists of the *thermodynamic perturbation* method.[34] We start from Eq. (21), and we write $Q_C(T,Z)$ for $Z+\delta Z$:

$$\begin{aligned}Q_C(T,Z+\delta Z)&=\int_{\Lambda'}\exp[-\beta V(\vec{R}',Z+\delta Z)]d^{3N-7}\vec{R}'\\&=Q_C(T,Z)\langle\exp-\beta[V(\vec{R}',Z+\delta Z)\\&\quad-V(\vec{R}',Z)]\rangle_Z,\end{aligned} \tag{25}$$

where the canonical average $\langle\rangle_Z$ is made with the constraint Z, at temperature T. This last equation immediately gives the derivative $\partial F_C/\partial Z$,

$$\frac{\partial F_C}{\partial Z}(T,Z)=\left\langle\frac{\partial V}{\partial Z}(\vec{R}',Z)\right\rangle_Z. \tag{26}$$

The building of the function F_C is then allowed by a simple integration,

$$F_C(T,Z)=F_C(T,Z_0)+\int_{Z_0}^{Z}\left\langle\frac{\partial V}{\partial Z}\right\rangle_Z dZ. \tag{27}$$

The quantity $\partial V/\partial Z$, calculated with Eq. (9), is recorded and averaged for several values of Z, and $F_C(T,Z)$ is then evaluated. This method is imprecise for two reasons. The averaging obviously introduces an error, and also the integration itself, since it is carried out with a limited amount of points (each of them requires a simulation). An alternative method for computing free-energy differences is the approach of Voter,[35] also known as the ''displacement vector'' method, or also the ''acceptance ratio'' method, from the precursor work of Bennett.[23,36] It is especially designed for the Monte Carlo scheme. To take account of the holonomic constraint Z in this procedure is theoretically easy, but practically not straightforward (some other formulations have been proposed[37]). Our presentation is close to the original formulation of Voter. The Metropolis function for a canonical ensemble is the acceptance probability for a Monte Carlo move causing an energy change ΔE; that is, $M_\beta(\Delta E)=\min(1,\exp(-\beta\Delta E))$. For any E and E', we have

$$\exp(-\beta E)M_\beta(E'-E)=\exp(-\beta E')M_\beta(E-E'). \tag{28}$$

Let us consider E and E' as functions of the coordinates $\vec{R}$ in the configurational space, and assume that $E=V(\vec{R}-\vec{D}/2)$, $E'=V(\vec{R}+\vec{D}/2)$, where V is a potential-energy function, $\vec{D}$ a constant vector of the configurational space. We have, for any $\vec{R}$ and $\vec{D}$, the following identity:

$$\begin{aligned}&\exp[-\beta V(\vec{R}-\vec{D}/2)]M_\beta[V(\vec{R}+\vec{D}/2)-V(\vec{R}-\vec{D}/2)]\\&\quad=\exp[-\beta V(\vec{R}+\vec{D}/2)]M_\beta[V(\vec{R}-\vec{D}/2)-V(\vec{R}+\vec{D}/2)]\end{aligned} \tag{29}$$

We multiply both left- and right-hand sides by the constraint $\delta[\xi(\vec{R})-Z]$, and we integrate over the configuration space $\Lambda=\{\vec{R}\}$,

$$I_- = \int_\Lambda e^{-\beta V_-(\vec{R})} M_\beta [V_+(\vec{R})-V_-(\vec{R})]\,\delta(\xi(\vec{R})-Z)\,d\vec{R}$$
$$= \int_\Lambda e^{-\beta V_+(\vec{R})} M_\beta [V_-(\vec{R})-V_+(\vec{R})]\,\delta(\xi(\vec{R})-Z)\,d\vec{R} = I_+ , \tag{30}$$

where we used the notation $V_\pm(\vec{R})=V(\vec{R}\pm\vec{D}/2)$. We shift the integration variable in I_-,

$$I_- = \int_\Lambda e^{-\beta V(\vec{R})} M_\beta [V(\vec{R}+\vec{D})-V(\vec{R})]$$
$$\times\,\delta[\xi(\vec{R}+\vec{D}/2)-Z]\,d\vec{R}. \tag{31}$$

Now ξ is linear in $\vec{R}$; therefore $\xi(\vec{R}+\vec{D}/2)=\xi(\vec{R})+\Delta Z/2$ with $\Delta Z=\xi(\vec{D})$. Hence

$$I_- = \int_\Lambda e^{-\beta V(\vec{R})} M_\beta [V(\vec{R}+\vec{D})-V(\vec{R})]\,\delta[\xi(\vec{R})-Z$$
$$+\Delta Z/2]\,d\vec{R}, \tag{32}$$

and a similar form for I_-. Our aim is to calculate the configurational free-energy difference $\Delta F_C=F_+-F_-$, with $F_\pm=-k_B T\,\ln\langle\delta[\xi(\vec{R})-(Z\pm\Delta Z/2)]\rangle=-k_B T\ln Q_\pm$. One has

$$\frac{Q_+}{Q_-}=\frac{I_-}{Q_-}\frac{Q_+}{I_+}=\frac{\langle M_\beta[V(\vec{R}+\vec{D})-V(\vec{R})]\rangle_-}{\langle M_\beta[V(\vec{R}-\vec{D})-V(\vec{R})]\rangle_+}, \tag{33}$$

with the notation

$$\langle A\rangle_\pm=\frac{\int_\Lambda A(\vec{R})e^{-\beta V(\vec{R})}\delta[\xi(\vec{R})-(Z\pm\Delta Z/2)]\,d\vec{R}}{\int_\Lambda e^{-\beta V(\vec{R})}\delta[\xi(\vec{R})-(Z\pm\Delta Z/2)]\,d\vec{R}}, \tag{34}$$

the average of the observable $A(\vec{R})$ over a canonical sampling with the constraint $\xi(\vec{R})=Z\pm\Delta Z/2$. Finally we can write the configurational free-energy difference between two configurations, held, respectively, with the constraint $Z+\Delta Z/2$ and $Z-\Delta Z/2$:

$$F_C(T,Z+\Delta Z/2)-F_C(T,Z-\Delta Z/2)=-k_B T\ln(Q_+/Q_-). \tag{35}$$

The configuration integral Q_+ (Q_-) is calculated by performing a Monte Carlo simulation governed by the potential function $V(\vec{R})$ with the constraint over $Z+\Delta Z/2$ ($Z-\Delta Z/2$), and by accumulating the average probability that a step from $\vec{R}$ to $\vec{R}+\vec{D}$ ($\vec{R}$ to $\vec{R}-\vec{D}$) would be accepted. These displacements, which make the system jump from a $Z+\Delta Z/2$ constraint to a $Z-\Delta Z/2$ constraint (or vice versa), are never really performed; only the acceptance probability is stored.

Thus, by carrying out several simulations at various intercluster distances $\{Z_i\}$, and by taking $\Delta Z=Z_{i+1}-Z_i$ as a constant, we can evaluate step by step directly (and not by integration) the free-energy differences $F_C(T,Z_{i+1})-F_C(T,Z_i)$. When the simulation with constraint Z_i is actually being performed, we store the three averaged following quantities: Q_+ by steps toward $Z_i+\Delta Z=Z_{i+1}$ to calculate the numerator of the right-hand side of Eq. (33), Q_- by steps from Z_i toward $Z_i-\Delta Z=Z_{i-1}$ to calculate the denominator at $Z=Z_{i-1}$; and $\langle\partial V/\partial Z\rangle_Z$ to achieve the thermodynamic perturbation formula.

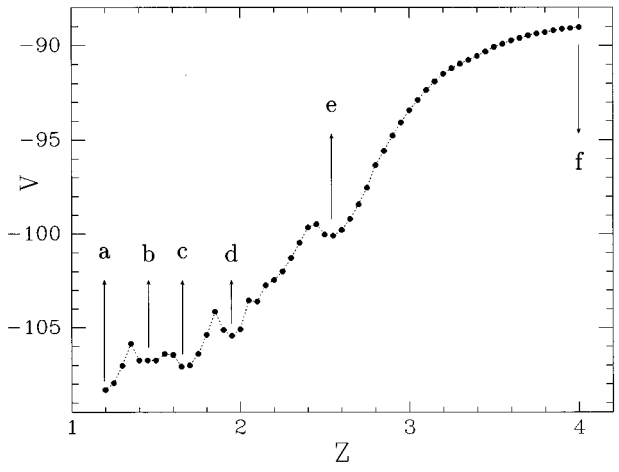

FIG. 1. Reference curve $V(Z)=F_C(T=0,Z)$ for the Lennard-Jones system $Ar_{13}+Ar_{13}$. The distance and energy units are LJ.

The resulting curves $F_C(T,Z)$ at fixed T still have an undetermined additive constant, which is provided here by the multiple histogram simulations at fixed Z. Therefore a complete determination of the (T,Z) map of the free energy can be achieved with differents sets of methods, employing the algorithms developed in the present and previous sections.

III. RESULTS FOR $Ar_{13}+Ar_{13}$

The testing of the methods presented in Sec. II was first performed on the $Ar_{13}+Ar_{13}$ dimer. The argon clusters were modeled by simple classical Lennard-Jones 6–12 potential, with parameters $\sigma=3.4$ Å and $\varepsilon/k_B=119.8$ K:

$$V(\{\vec{r}_i\})=\sum_{i<j} 4\varepsilon\left[\left(\frac{\sigma}{r_{ij}}\right)^{12}-\left(\frac{\sigma}{r_{ij}}\right)^{6}\right]. \tag{36}$$

The use of reduced units $\varepsilon=\sigma=1$ in the following allows us to describe these systems as well as other rare gases, though with different parameters σ and ε.[38] The time step in MD simulations was chosen as $\Delta t=0.01$ LJ units. Such a time step leads to the conservation of the total energy within 10^{-5} (relatively) for simulations of 2×10^5 time steps.

Each Ar_{13} cluster has the I_h ground geometry of a perfect icosahedron with a central atom, and a binding energy $V_{13}=-44.327\varepsilon$, whereas the compact Ar_{26} is known to exhibit a C_{2v} structure, with an energy $V_{26}=-108.316\varepsilon$.[1,39] The reference curve of the energy minima versus the intercluster separation Z is plotted on Fig. 1, for $1.2\leqslant Z/\sigma\leqslant 4.0$. One interesting feature is the existence of a long-distance minimum [named isomer (e)] at $Z=2.53\sigma$ separated by a small barrier from a series of minima corre-

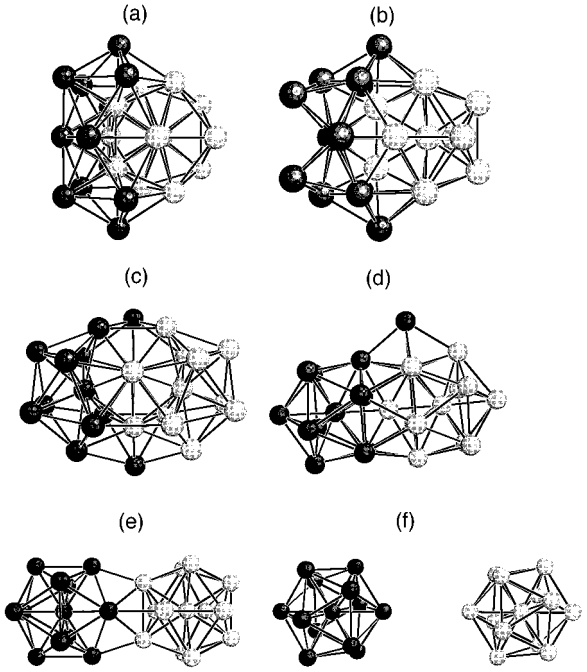

FIG. 2. Six snapshots of locally stable Ar_{26} with the Z constraint, on the reference curve $T=0$. Isomer (a) $Z=1.20\sigma$, $V=-19.66\varepsilon$ (C_{2v} compact structure). Isomer (b) $Z=1.49\sigma$, $V=-18.09\varepsilon$. Isomer (c) $Z=1.67\sigma$, $V=-18.42\varepsilon$. Isomer (d) $Z=1.95\sigma$, $V=-16.78\varepsilon$. Isomer (e) $Z=2.53\sigma$, $V=-11.47\varepsilon$. Isomer (f) $Z=4.0\sigma$, $V=-0.38\varepsilon$. All structures except (f) are stable without the Z constraint.

sponding to more compact configurations. The geometries of the asymptotic configurations $Z=1.2\sigma$ and $Z=4.0\sigma$, named isomers (a) and (f), as well as the geometry of the long distance minimum, are plotted in Fig. 2. This reference curve also shows three particularly stable structures, the first one [isomer (b)] being located at $Z=1.49\sigma$, the second one (isomer c) at $Z=1.67\sigma$, and the last one [isomer (d)] at $Z=1.95\sigma$. These isomers are shown on the same figure as isomers (a), (e), and (f).

The existence of an energy barrier between both clusters near $Z\simeq 2.43\sigma$ which separates the compact structures from the stable prolate $Ar_{13}+Ar_{13}$ can be investigated further with an adequate search of the saddle point configuration on the PES. This configuration was investigated by systematically searching for the maximal value of V and minimal value of $|\partial V/\partial Z|$ after relaxation of all others degrees of freedom. Its energy is about -10.0 units with respect to $V(Z=\infty)=0$, so one could certainly not hope to locate the dimer in the prolate structure with a frontal collision process. The numerous irregularities of the $V(Z)$ curve for $Z<2.5\sigma$ are mainly due to that one can explore numerous discrete minima compatible with the constraint which may be separated by higher saddle points, and also to the fact that we did not practically let both clusters mix together, the atoms of each cluster always remaining connected to their respective c.o.m.

The reference curve $F_C(T,Z)$ at fixed Z was calculated with the constrained multiple histogram method described above, for the maximal $Z=4.0\sigma$, and in the range $0.01\leqslant T\leqslant 0.5$ LJ units. Both MD and MC algorithms were used to extract the configurational density of states and the

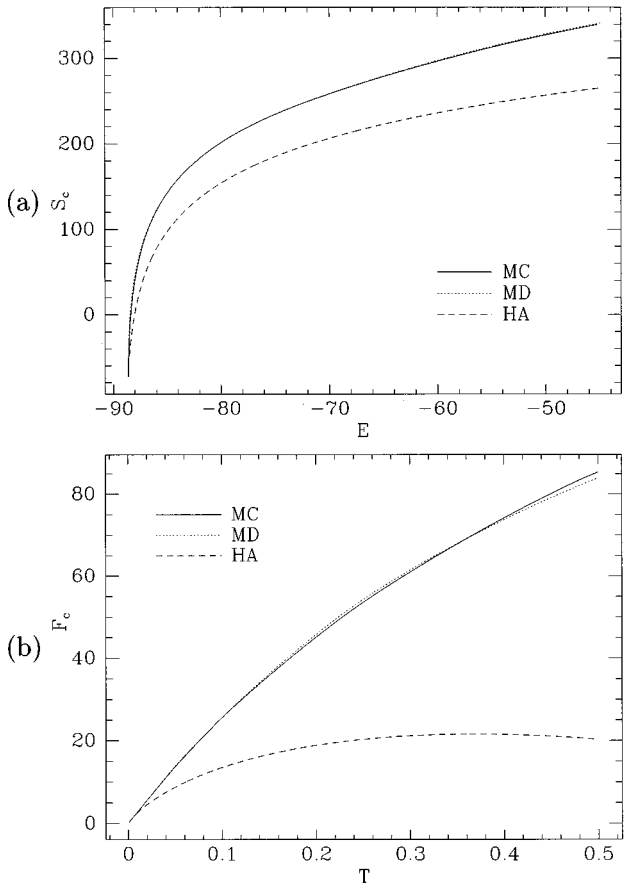

FIG. 3. Reference curves $S_C(V,Z)$ and $F_C(T,Z)$ both calculated with the constrained multiple histogram method at $Z=4.0\sigma$. Three curves are plotted, extracted from MC and MD simulations and in the harmonic origin approximation (HA). (a) Microcanonical configurational entropy $S_C(V,Z)$. (b) Canonical configurational free energy $F_C(T,Z)$.

partition function of this system. At the lowest temperatures $T<0.05$, the obtained curve was extended and fitted to a $T\ln T$ function, as would be obtained in the harmonic approximation. The added points were then discarded, leaving just the original curve with now the reference $F_C(T,0)=0$. We have also calculated the microcanonical configurational entropy $S_C(V,Z)$ with both methods, which was fitted to a $(3N-8)\ln V$ function for the lowest V. The results for both methods are plotted in Fig. 3 and are nearly superposed, which warrants us on the quality of the performed sampling.

In Fig. 4, we plotted several $F(T,Z)$ curves at finite temperature calculated with both thermodynamic perturbation and displacement-vector methods. The agreement between these two techniques is very good in the whole range $0.01\leqslant T\leqslant 0.5$. The complete (T,Z) map of the free energy with the reference $F(0,\infty)=0$ is plotted on Fig. 5. For temperatures less than about 0.2 LJ units, isomers (b), (d), and (e) remain metastable, but (e) has clearly the greater basin of attraction. When T reaches 0.2, the barrier which separates (e) and the more compact shapes disappear, and only (b) and (d) are metastable, until $T\sim 0.3$. At last, only the compact shape (a) is stable when T goes over 0.3. Moreover, in the range $0.2<T<0.3$, isomer (b) seems to be slightly stabilized as compared to $T<0.2$.

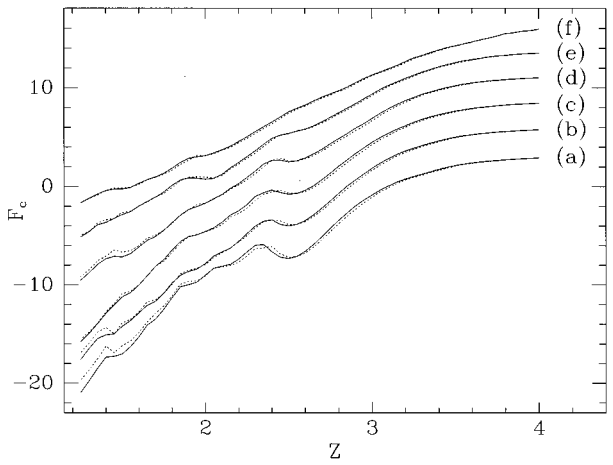

FIG. 4. Finite-temperature $F_C(T,Z)$ curves calculated with the thermodynamic perturbation (solid lines) and the displacement-vector (dashed lines) methods. The free-energy reference is $F_C(T=0,\ Z=\infty)=0$. (a) $T=0.05$. (b) $T=0.10$. (c) $T=0.15$. (d) $T=0.20$. (e) $T=0.25$. (f) $T=0.30$ LJ units.

The global effect of the temperature on the free energy curves is a general smoothing of the potential-energy curve. Figure 5, which represents the $F(T,Z)$ surface, allows us to visualize this effect better. In the present case, one can observe the vanishing of the stability of the various metastable isomers at low T, but also the stabilization of an isomer (b) in a particular range of temperatures. The quasidisappearance of the Z structuration of the $F(T,Z)$ surface around $T\simeq 0.3$–0.4 is to be related to the known melting temperature of argon clusters in this size range, namely, $T\simeq 0.30$.[40]

IV. RESULTS FOR Na_8+Na_8

The potential energy of sodium clusters was calculated using a distance-dependent tight-binding (DDTB) Hamiltonian developed by Poteau and Spiegelmann,[4] and which can be written as

$$\hat{h}=\sum_{i,j} h_{ij}a_i^{\dagger}a_j, \tag{37}$$

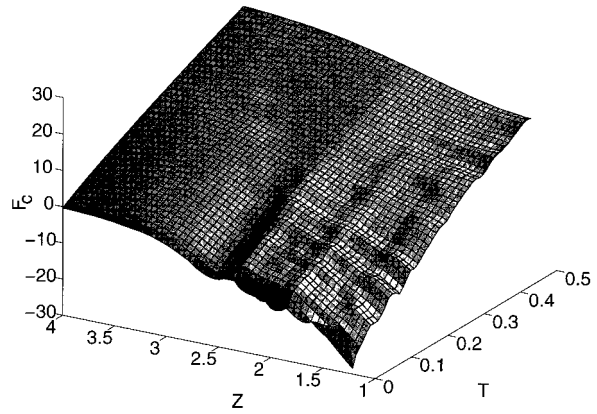

FIG. 5. $F_C(T,Z)$ map of the configurational free energy with the reference $F_C(0,\infty)=0$ for the $Ar_{13}+Ar_{13}$ dimer. The units are LJ.

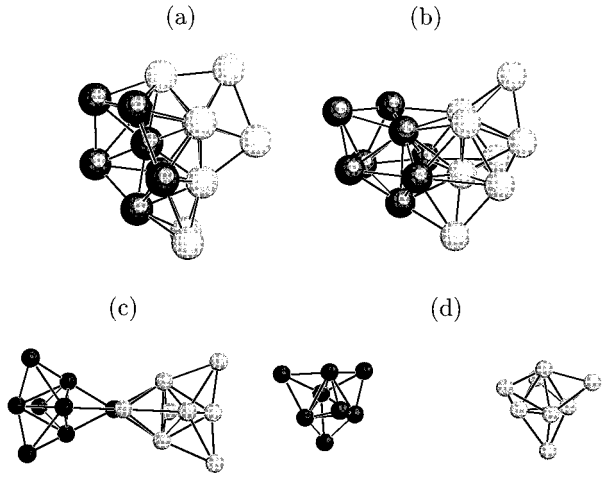

FIG. 6. Four snapshots of locally stable Na_{16} with the Z constraint, as part of the reference curve $T=0$. Isomer (a) $Z=6.25$ bohr, $V=-1.3586$ eV. Isomer (b) $Z=9.25$ bohr, $V=-1.1367$ eV. Isomer (c) $Z=14.25$ bohr, $V=-0.4446$ eV. Isomer (d) $Z=26.25$ bohr, $V=-8.2\times 10^{-5}$ eV. The first structure (a) is the C_1 compact structure.

where $a_i^{\dagger}$ and a_j, respectively, are creation and annihilation operators corresponding to an s orbital on site i and j of the cluster. Not only are the s atomic orbitals taken into account in this Hamiltonian, but also the effect of p orbitals which is included as a perturbation to the matrix elements:

$$h_{ii}=h_{ii}^{(0)}+h_{ii}^{(2)}=\sum_{k\neq i}^{\text{atoms}}\left[\rho_{ss}(r_{ik})-\frac{t_{s\sigma}^2(r_{ik})}{\varepsilon_{3p}-\varepsilon_{3s}}\right], \tag{38}$$

$$h_{ij}=h_{ij}^{(0)}+h_{ij}^{(2)} =t_{ss}(r_{ij})-\sum_{k\neq i,j}^{\text{atoms}}\left[\frac{t_{s\sigma}(r_{ik})t_{s\sigma}(r_{jk})}{\varepsilon_{3p}-\varepsilon_{3s}}\times\frac{\vec{r}_{ij}\cdot\vec{r}_{jk}}{\|\vec{r}_{ik}\|\|\vec{r}_{jk}\|}\right], \tag{39}$$

with $\rho_{ss}(r)$, $t_{ss}(r)$, and $t_{s\sigma}(r)$, respectively, ion-ion repulsion, s–s, and s–p_σ transfer integrals taken as functions of the internuclear distance. These functions were fitted on *ab initio* curves for Na_2 and Na_4.[4] Being given a geometrical configuration of the cluster nuclei, the ground-state potential energy is calculated as the sum of the one-electron energies

$$V=\sum_{i\in occ} n_i\varepsilon_i, \tag{40}$$

where ε_i are the eigenvalues of the DDTB Hamiltonian, and n_i the occupation numbers. Due to the larger computer time needed to compute this energy function, we had to reduce the amount of statistical sampling points by a factor 10 with respect to the simulations of LJ clusters. Only the MC simulations scheme was used here to calculate $F_C(T,Z)$.

The Na_8 and Na_{16} ground structures according to this energy function are represented in Fig. 6. Na_8, with the energy -4.95 eV, has T_d symmetry, whereas Na_{16}, in its compact triaxial shape (axial ratios $X_0=0.27$, $Y_0=0.33$, and $Z_0=0.40$), has a binding energy of -11.26 eV and C_1 symmetry. The reference curve at $T=0$ is plotted in Fig. 7. Con-

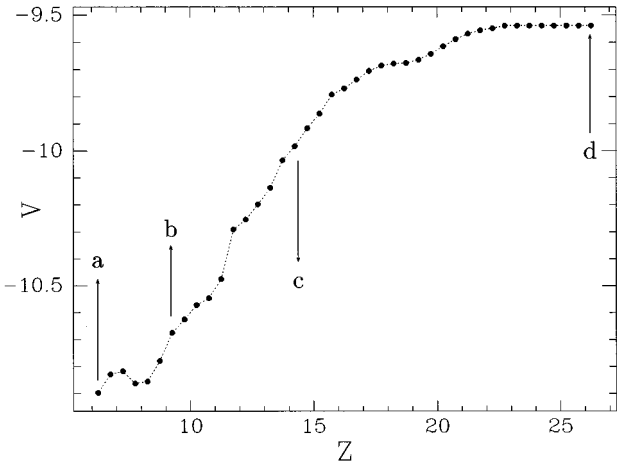

FIG. 7. Reference curve $V(Z)=F_C(T=0,Z)$ for the sodium dimer Na_8+Na_8, with respect to infinitely distant clusters. The distance units are bohr, the energy units are eV.

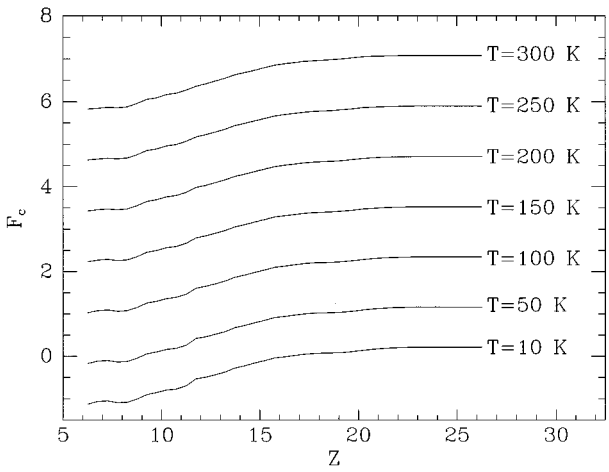

FIG. 8. Finite-temperature $F_C(T,Z)$ curves calculated with the displacement-vector method. The free-energy reference is $F_C(T=0,\ Z=\infty)=0$.

trary to the rare-gas case, it does not clearly exhibit any metastable prolate structure or local barrier between such a structure and a more compact isomer. Also, the irregularities at small Z do not seem very apparent here, and rather more smooth with respect to the argon case. This might be due to the use of a quantal Hamiltonian and to the physically nonlocal character of the interaction in metal clusters.

The agreement between the thermodynamic perturbation and displacement-vector methods was again rather good. Several curves $F_C(T,Z)$ of the configurational Helmholtz free energies are plotted in Fig. 8, with the reference $F(T=0,\ Z=\infty)=0$, at different temperatures 10 K $<T<$300 K. There is no evidence on this plot for any appearance of a locally stable isomer at some Z. The only stable isomer is the compact Na_{16}, and no intermediate structure is stabilized by either temperature or entropic effects. We did not see any qualitative difference at higher temperatures 300 K$<T<$600 K.

V. DISCUSSION AND CONCLUSION

We have implemented and checked several methods to determine the Helmholtz free-energy function in constrained problems, corresponding here to the mutual approach of two clusters. We have tested on this problem the convergency of both Monte Carlo and molecular-dynamics simulations, which was found to be quite satisfactory as in a previous study[19] dealing with phase transitions in clusters. Again, as already mentioned above, we observe that, for the same result and equivalent sampling, MC-based algorithms appear to be more efficient when considering the computer-time criterion.

Also, a good stability of the results was obtained when comparing the thermodynamic perturbation algorithm versus the displacement-vector approach. However, whereas the thermodynamic perturbation method had been up to now essentially combined with MD, the formalism of the displacement-vector method makes it directly suited for the MC scheme. Here we have shown that the thermodynamic perturbation method can also be very efficient when combined with the MC method. From the methodological point of view, the present study is not only concerned with applications in cluster physics, but should also stimulate similar studies in the field of finite-temperature reactivity, particularly for biomolecules.

However, it is to be noted that the implementation of the present algorithms (especially the multiple histogram methods) was made practical due to the linear character of the involved constraint. Its extension to the general case of nonlinear constraints still demands further analytical work.

As concerns the present applications to the interaction between cluster entities, the results clearly indicate in the case of $Ar_{13}+Ar_{13}$ that possible metastable dimerlike configurations, like local minima of the free energy, exist at low temperature, although they are not likely to be stabilized in a two-body frontal approach. At higher finite temperature, however, those minima tend to vanish, and a single stable compact isomer remains. Beyond the frontal approach, it should be interesting to extend the present study to include centrifugal contributions, which is not quite straightforward in the Monte Carlo scheme.[41]

As concerns the interaction between two Na_8 clusters, the low-temperature free energy does not present any evidence of a dimerized isomer of Na_{16}, and this result is almost independent of temperature. Independently of the Z constraint considered here, the present work can also be viewed as a contribution that incorporates entropic effects for studying the stability and structure of clusters and other complex molecular systems at finite temperature.

ACKNOWLEDGMENTS

Support by the CNRS, the Région Midi-Pyrénées, the Université Paul Sabatier, and the MESR is gratefully acknowledged. The authors are especially grateful to J. Durup and P. Labastie for helpful discussions. F. C. also thanks ENSL for supporting research possibilities.

[1] J. Farges, M.-F. De Feraudy, B. Raoult, and G. Torchet, Surf. Sci. **156**, 370 (1985).
[2] J. A. Northby, J. Chem. Phys. **87**, 6166 (1987).
[3] U. R othlisberger and W. Andreoni, Z. Phys. D **20**, 243 (1991).
[4] R. Poteau and F. Spiegelmann, Phys. Rev. B **45**, 1878 (1992); J. Chem. Phys. **98**, 6450 (1993).
[5] S. Saito and S. Ohnishi, Phys. Rev. Lett. **59**, 190 (1987); Y. Ishii, S. Saito, and S. Onishi, Z. Phys. D **7**, 289 (1987); S. Saito and M. L. Cohen, Phys. Rev. B **38**, 1123 (1988); M. Nakamura, Y. Ishii, A. Tamura, and S. Sugano, Z. Phys. D **19**, 145 (1991).
[6] O. Knospe, R. Schmidt, E. Engel, U. R. Schmidt, R. M. Dreizler, and H. O. Lutz, Phys. Lett. A **183**, 332 (1992) ; R. Schmidt and H. O. Lutz, *ibid.* **183**, 338 (1993).
[7] B. Montag and P. G. Reinhard, Phys. Lett. A **193**, 380 (1994).
[8] Y. Yannouleas and U. Landman, Phys. Rev. B **51**, 1902 (1994).
[9] G. Lauritsch, P. G. Reinhard, J. Meyer and M. Brack, Phys. Lett. A **160**, 179 (1991); M. Brack, Rev. Mod. Phys. **65**, 677 (1993).
[10] R. Schmidt, G. Seifert, and H. O. Lutz, Phys. Lett. A **158**, 231 (1991); G. Seifert, R. Schmidt, and H. O. Lutz, *ibid.* **158**, 237 (1991).
[11] F. S. Zhang, E. Suraud, F. Spiegelmann, V. Frayssé, F. Chatelin, and R. Glowinski, Z. Phys. D **35**, 131 (1995).
[12] F. S. Zhang, F. Spiegelmann, E. Suraud, V. Frayssé, R. Poteau, R. Glowinski, and F. Chatelin, Phys. Lett. A **193**, 75 (1994).
[13] R. S. Berry, J. Jellinek, and G. Natanson, Phys. Rev. A **30**, 919 (1984); J. Jellinek, T. L. Beck, and R. S. Berry, J. Chem. Phys. **84**, 2783 (1986); H. L. Davis, J. Jellinek, and R. S. Berry, *ibid.* **86**, 6456 (1987); D. J. Wales and R. S. Berry, *ibid.* **92**, 4283 (1990); Phys. Rev. Lett. **73**, 2875 (1994).
[14] A. Bulgac and D. Kusnezov, Phys. Rev. B **45**, 1988 (1992).
[15] R. Poteau, F. Spiegelmann, and P. Labastie, Z. Phys. D **30**, 57 (1994).
[16] J. P. K. Doye and D. J. Wales, J. Chem. Phys. **102**, 9659 (1995).
[17] F. Spiegelmann and D. Pavolini, *ibid.* **89**, 4954 (1988); V. Bonacic-Koutecky, P. Fantucci, and J. Koutecky, Phys. Rev. B **37**, 4369 (1988).
[18] R. Car and M. Parrinello, Phys. Rev. Lett. **55**, 2471 (1985).
[19] F. Calvo and P. Labastie, Chem. Phys. Lett. **247**, 395 (1995).
[20] J.-P. Ryckaert and G. Ciccotti, Mol. Phys. **58**, 1125 (1986).
[21] S. Nosé, Mol. Phys. **52**, 255 (1984); J. Chem. Phys. **81**, 511 (1984).
[22] J.-P. Valleau and D. N. Card, J. Chem. Phys. **57**, 5457 (1972).
[23] D. Frenkel, in *Computer Simulation in Material Science*, edited by M. Meyer and V. Pontikis (Kluwer, Dordrecht, 1991), pp. 85–117.
[24] E. A. Carter, G. Ciccotti, J. T. Hynes, and R. Kapral, Chem. Phys. Lett. **156**, 472 (1989).
[25] E. Paci, G. Ciccotti, M. Ferrario, and R. Kapral, Chem. Phys. Lett. **176**, 581 (1991).
[26] J.-M. Depaepe, J.-P. Ryckaert, E. Paci, and G. Ciccotti, Mol. Phys. **79**, 515 (1993).
[27] W. H. Press, B. P. Flannery, S. A. Teukolsky, and W. T. Vetterling, *Numerical Recipes* (Cambridge University Press, Cambridge, 1987).
[28] J. Durup and F. Alary, in *Modelling of Biomolecular Structures and Mechanisms*, edited by A. Pullman *et al.* (Kluwer, Dordrecht, 1995), pp. 167–180.
[29] M. P. Allen and D. J. Tildesley, *Computer Simulations of Liquids* (Oxford University Press, London, 1987).
[30] N. Metropolis, A. Rosenbluth, M. N. Rosenbluth, A. Teller, and E. Teller, J. Chem. Phys. **21**, 1087 (1953).
[31] P. Labastie and R. L. Whetten, Phys. Rev. Lett. **65**, 1567 (1990).
[32] C. J. Tsai and K. D. Jordan, J. Chem. Phys. **99**, 6957 (1993).
[33] S. Weerasinghe and F. G. Amar, J. Chem. Phys. **98**, 4967 (1993).
[34] M. R. Mruzik, F. F. Abraham, D. E. Schreiber, and G. M. Pound, J. Chem. Phys. **64**, 481 (1976).
[35] A. F. Voter, J. Chem. Phys. **82**, 1890 (1985).
[36] C. H. Bennett, J. Comput. Phys. **22**, 245 (1976).
[37] D. J. Tobias and C. L. Brooks III, Chem. Phys. Lett. **142**, 472 (1987).
[38] J.-P. Hansen and I. R. Mc Donald, *Theory of Simple Liquids* (Academic, New York, 1986).
[39] A. L. Mackay, Acta Crystallogr. **15**, 916 (1962).
[40] F. Calvo and P. Labastie, Chem. Phys. Lett. **248**, 233 (1996).
[41] F. Calvo and P. Labastie (unpublished).